(Received 24 August 2023, Accepted 29 November 2023, Scheduled 3 December 2023)

Frequency Diversity Arc Array with Angular Broadening Null Steering for Sidelobe Suppression

Ying Tian[1, 2, *], Wei Xu[1, 2], Pingping Huang[1, 2], Weixian Tan[1, 2], and Yaolong Qi[1, 2]

[1] College of Information Engineering, Inner Mongolia University of Technology, Hohhot, China
[2] Inner Mongolia Key Laboratory of Radar Technology and Application, Hohhot, China

ABSTRACT: The structure of the frequency diversity arc array (FDAA) is a circular arc, which can achieve fast scanning in all directions and large viewing angles. By selecting the appropriate array elements for FDAA to form an effective working array and designing the symmetrical logarithmic frequency offset, a more aggregated point-like beam pattern is obtained. However, due to the structural characteristics of FDAA, the anti-density weighting phenomenon is generated, which limits the application of FDAA in radar system for target recognition and tracking. In order to solve the problem of high sidelobe of FDAA caused by inverse density weighting, a method of FDAA with angle widening null guidance for sidelobe suppression is proposed in this paper. The linear constraint minimum variance (LCMV) criterion is used to set zero points at a fixed position in the direction of interference, so that the interference is in a null with a certain width. Through Matlab simulation, it is verified that this method has a certain effect on suppressing FDAA sidelobe interference.

1. INTRODUCTION

Frequency diverse array (FDA) is a new type of radar system first proposed by Antonik et al. in 2006 [1]. The beam pattern obtained by a traditional phased array (PA) is angle-dependent but distance-independent [2]. The essence of FDA is to introduce a small frequency increment between adjacent array elements of traditional phased array radar. This characteristic makes the radar pattern change from the angle coupling characteristic of phased array to the two-dimensional coupling characteristic of distance-angle, so it can form a space beam pattern with dual dependence of distance-angle dimension. FDA has obtained the degree of freedom of distance control, which makes signal processing more flexible. FDA has extensive research value in beamforming and interference suppression [3–5].

In recent years, FDA has received extensive attention and in-depth research from many researchers. In terms of beamforming methods, in [6], the influence of large frequency offset on FDA beam characteristics was studied. In [7], a linear frequency diversity array based on logarithmic function increasing frequency offset is proposed. By destroying the mutual coupling period characteristics of FDA, the false main lobes other than the target main lobe are effectively suppressed. Subsequently, scholars have done a lot of exploration on nonlinear frequency offset design, such as applying square and cubic frequency offset [8], sinusoidal frequency offset [9], arctangent frequency offset [10], Taylor window frequency offset [11], and random logarithm frequency offset [12] to FDA. These frequency offset design methods have improved the beam energy focusing and positioning performance in the range-angle dimension target azimuth. This idea provides a certain reference value for the frequency offset optimization theory. In addition, many scholars have studied clutter interference suppression. A method of using simulated annealing algorithm to optimize the frequency offset parameters of linear frequency diversity array was proposed in [13] to achieve the range-angle low sidelobe comprehensive beam effect. In [14], the adaptive beamforming is studied by using the angle-distance two-dimensional coupling relationship of FDA, which improves the anti-interference performance of the system. The use of convex optimization to optimize the optimal weight of each array element transmitting waveform is proposed in [15], which not only focuses energy on the target point, but also reduces the sidelobe. In [16], a range angle localization algorithm based on Cramer-Rao lower bound (CRLB) minimization for FDA and multiple-input multiple-output (MIMO) radar is proposed. In [17], an FDA symmetric beam pattern with nonuniform frequency offset and density weighted algorithm is proposed, which reduces the sidelobe level in both distance and angle dimensions. A deterministic method for three-dimensional synthesis of antenna arrays considering far-field pattern reconfiguration, polarization setting, dynamic range ratio reduction, and near-field control is proposed in [18]. In [19], an anti-jamming method based on non-adaptive beamforming for FDA-MIMO radar system is proposed, which can effectively suppress the main-lobe deception jamming problem. In order to effectively improve the isolation and null depth at low elevation angles, in [20], a design of an arc antenna array with high isolation was proposed. However, with the continuous research on the traditional FDA, it is found that the traditional FDA scanning range has certain limitations. In [21], the structure of the traditional FDA was innovated, and the concept of frequency diversity arc array (FDAA) was proposed. FDAA designs the array structure as an arc, which not only inherits the advantages of FDA, but also achieves the purpose of wide coverage and all-round beam

* Corresponding author: Ying Tian (20211100100@imut.edu.cn).

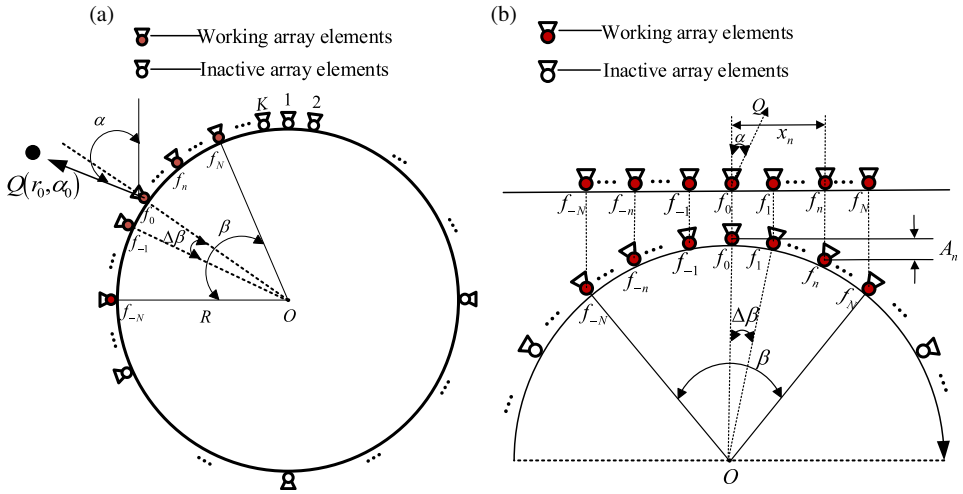

FIGURE 1. Structural model of FDAA.

scanning [22]. Subsequently, an FDAA beam pattern based on both symmetric logarithmic frequency offset and amplitude weighting was proposed in [23], and a more clustered point beam was obtained. The higher sidelobes around the main lobe were also suppressed.

Although FDAA can achieve large-angle, all-round 360° beam scanning, the array elements on the arc are arranged at equal angle intervals, which will lead to the problem of inverse density weighting, resulting in relatively high sidelobes. Sidelobe suppression of FDAA at a fixed distance is the main trend of future research on FDAA. In this paper, by analyzing the beam pattern of FDAA, it is found that the sidelobes are 'X'-shaped and mainly concentrated in a certain area. In order to suppress the sidelobes at a fixed position, an angle-widened null steering FDAA is proposed for sidelobe suppression. The method broadens the nulls in any interference direction in the angle domain to reduce the influence of the interference signal on the main lobe beam and suppress the sidelobe level.

There are five sections in this paper. The second section introduces the geometric structure model of FDAA and designs the nonlinear frequency offset by applying the symmetric logarithm of different coefficients to FDAA. In the third section, the sidelobe characteristics of the beam pattern of FDAA are analyzed, and the linear constrained minimum variance (LCMV) criterion is used to suppress the sidelobe of the fixed interference position of FDAA based on the symmetric logarithmic frequency offset. In the fourth section, the influence of different coefficients on the FDAA spot beam is analyzed by Matlab simulation, and the sidelobe suppression effect of FDAA's angle domain widening null shaping based on symmetrical logarithmic frequency offset design is verified. The fifth section summarizes the full text.

2. FDAA BEAM SYNTHESIS

2.1. FDAA Structure Model

Figure 1 shows the structure model of FDAA. Figure 1(a) is the planar diagram of FDAA, and Figure 1(b) is the equivalent linear array diagram of FDAA. FDAA is a circular structure composed of K array elements arranged evenly at equal angles, and the radius is represented by R. According to the scanning characteristics of each array element in FDAA, a single array element can only play a role in the gain of the main beam of the array within a certain range. Therefore, for targets in different directions, it is necessary to use the feed network system to select the appropriate array elements to form an activated array for beam scanning. Assuming that the aperture angle of the activated working array elements in FDAA is β and that the angle between adjacent array elements in FDAA is represented by $\Delta\beta$, the number of activated array elements K_A can be expressed as:

$$K_A = 2 \cdot \left\lfloor \frac{\beta}{2 \cdot \Delta\beta} \right\rfloor + 1 = 2N + 1 \tag{1}$$

where $\lfloor \cdot \rfloor$ is the rounding operation, and K_A is an odd number.

2.2. FDAA Beampattern Synthesis Analysis with Nonlinear Frequency Offset

As shown in Figure 1, the activated working array elements are $2N + 1$. It is assumed that α is the angle between the target point Q and the north direction, and the value range of α is (0°, 360°). The array element in the north direction is selected as the reference array element f_0. The phase compensation between a single activated array element forming an equal phase plane and the reference array element f_0 is:

$$\Delta\beta_{1,n} = \frac{2\pi f_c R}{c} \cdot A_n = \frac{2\pi f_c R}{c} \cdot [1 - \cos(n \cdot \Delta\beta)] \tag{2}$$

Here, A_n denotes the spatial distance difference between the nth array element and the reference array element f_0; c denotes the speed of light; and f_c denotes the carrier frequency.

Due to the coupling problem between the range-angle domain of FDAA, it is necessary to design a nonuniform frequency increment to make the beam pattern of FDAA approximately present as a point beam pattern. In this paper, the sym-

metric logarithmic function is used to design the nonlinear frequency offset. Assuming that the carrier frequency is expressed by f_c, the radiation frequency of the nth array element is expressed as:

$$f_n = f_c + \Delta f_n \quad n = -N, \cdots, 0, \cdots, N \tag{3}$$

The frequency offset Δf_n of the nth array element is represented by the symmetric logarithm of different coefficients, then Δf_n can be expressed as:

$$\Delta f_n = \Delta f \cdot \ln(q \cdot |n| + 1) \tag{4}$$

Here q represents the scale coefficient, and the different values of q represent the different frequency offset Δf_n of the design. In order to make the beamwidth formed by FDAA consistent, it is necessary to equal the frequency offset when n takes the maximum value. In this paper, different scale coefficients $q = 1$ and $q = 10$ are analyzed, and the corresponding fixed frequency offset constant Δf is two different values represented by Δf^1 and Δf^{10}. Then, Δf_n can be expressed as:

$$\Delta f_n = \begin{cases} \Delta f^1 \cdot \ln(|n| + 1) \\ \Delta f^{10} \cdot \ln(10 \cdot |n| + 1) \end{cases} \tag{5}$$

At the far-field target point Q, the transmitted signal $W_n(t)$ of the nth array element is expressed as:

$$W_n(t) = a_n \exp(j2\pi f_n t) \quad 0 \le t \le T \tag{6}$$

Here, a_n represents the complex weighting vector of the nth transmitted signal. The horizontal distance between the far-field target point Q and the nth array element can be approximately expressed as follows:

$$r_n \approx r_0 - x_n \sin\alpha_0 = r_0 - R\sin(n\Delta\beta) \cdot \sin\alpha_0 \tag{7}$$

where r_0 represents the target distance; α_0 represents the target angle; $f_c \gg \Delta f_n$; then the signal at the target point Q can be expressed as:

$$\begin{aligned} W(t, r_0, \alpha) = & \sum_{n=-N}^{N} W_n\left(t - \frac{r_n}{c}\right) \\ \approx & \exp\left[j2\pi f_c\left(t - \frac{r_0}{c}\right)\right] \sum_{n=-N}^{N} a_n \\ & \exp\left[j2\pi\Delta f_n\left(t - \frac{r_0}{c}\right)\right] \\ & \exp\left[j2\pi f_c \frac{R\sin(n\cdot\Delta\beta)\sin\alpha}{c}\right] \end{aligned} \tag{8}$$

At the desired position (r_0, α_0), the complex weighted vector a_n is:

$$\begin{aligned} a_n = & \exp\left[j2\pi\left(\frac{\Delta f_n r_0}{c} - \frac{f_c R\sin(n\cdot\Delta\beta)\sin\alpha_0}{c}\right.\right. \\ & \left.\left. - \frac{f_c R[1-\cos(n\cdot\Delta\beta)]}{c}\right)\right] \end{aligned} \tag{9}$$

The array factor (AF) of FDAA after applying a symmetric logarithmic nonlinear frequency offset is:

$$\begin{aligned} \mathrm{AF}(t, r_0, \alpha) = & \sum_{n=-N}^{N} a_n \exp\left[j2\pi\Delta f_n\left(t - \frac{r}{c}\right)\right] \\ & \exp\left[j2\pi f_c \frac{R\sin(n\cdot\Delta\beta)\sin\alpha}{c}\right] \end{aligned} \tag{10}$$

3. SIDELOBE SUPPRESSION

3.1. Analysis of Sidelobe Distribution of FDAA Beam Pattern

As shown in Figure 2, when the total number of activated array elements $K_A = 33$, and the FDAA beam pattern with the nonlinear frequency offset scale coefficient $q = 1$, it can be seen that the center position of the formed FDAA beam pattern forms a clear point beam pattern, and the sidelobes of the FDAA are mainly distributed in the angle-distance domain. There is a correspondence between any position in the distance domain and the position in the angle domain.

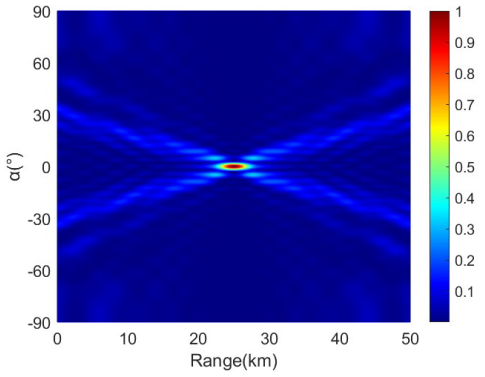

FIGURE 2. FDAA beam pattern with nonlinear frequency offset scale factor $q = 1$.

3.2. Angle Broadening Null Beamforming Method for FDAA

In this section, the linear constrained minimum variance criterion is used to form a null in a fixed direction to suppress the interference signal and reduce the sidelobe level. According to the linear constraint minimum variance criterion, it is known that the expected signal position is at α_0, and it is assumed that the null position is set at α_i, where α_i is an arbitrary value that is not equal to α_0, and the number of nulls $I < 2N$. The obtained constraint matrix and constraints are:

$$S = [\theta(\alpha_0)\ \theta(\alpha_i)] \tag{11}$$

$$\begin{cases} w^H\theta(\alpha_0) = 1 \\ w^H\theta(\alpha_i) = 0 \end{cases} \tag{12}$$

Here,

$$w^H = \sum_{n=-N}^{N} a_n \exp\left[j2\pi\Delta f \cdot \ln(|n|+1)\left(t - \frac{r}{c}\right)\right] \tag{13}$$

TABLE 1. Simulation parameter design.

Parameters	Symbol	Value
Frequency offset	Δf	30 kHz/16.73 kHz
Carrier frequency	f_c	10 GHz
Array element spacing	l_c	0.015 m
element amount	K	100
Number of activated array elements	K_A	33/67
Angle of array	β	$5\pi/12$
Array radius	R	0.378 m
Target distance	r_0	25 km
Target angle	α_0	0°

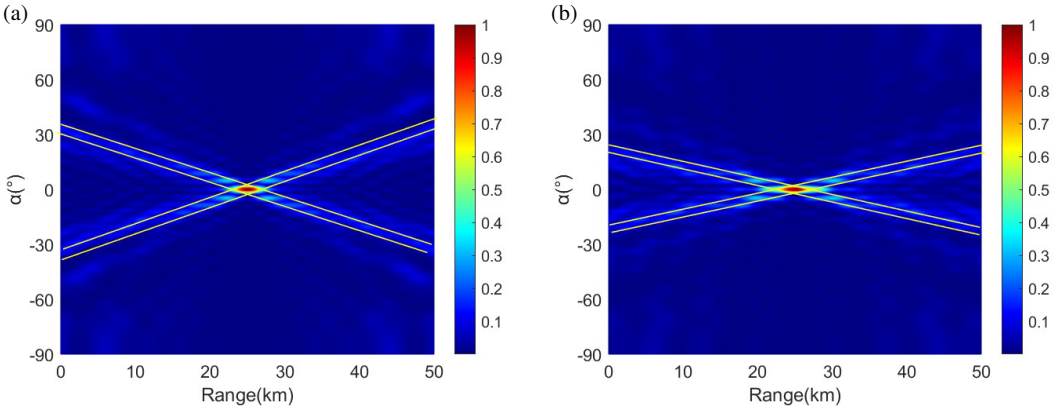

FIGURE 3. When $K_A = 33$, the influence of the scale coefficient q of the Sym-Log on the FDAA beam pattern.

$$\theta(\alpha_0) = \exp\left[j2\pi f_c \frac{R\sin((-N)\cdot\Delta\beta)\sin\alpha_0}{c}\right], ..., 1, ..., \exp\left[j2\pi f_c \frac{R\sin(N\cdot\Delta\beta)\sin\alpha_0}{c}\right] \quad (14)$$

$$\theta(\alpha_i) = \exp\left[j2\pi f_c \frac{R\sin((-N)\cdot\Delta\beta)\sin\alpha_i}{c}\right], ..., 1, ..., \exp\left[j2\pi f_c \frac{R\sin(N\cdot\Delta\beta)\sin\alpha_i}{c}\right] \quad (15)$$

In the formula, $i = -N, ..., 0, ..., N$.

According to the Lagrange multiplier method, the optimal weight vector is:

$$w_{\text{opt}} = \frac{S^{-1}\theta(\alpha_0)}{\theta^H(\alpha_0)S^{-1}\theta(\alpha_0)} \quad (16)$$

Then, the complex weighted vector a'_n that forms a null at the interference position α_i is:

$$a'_n = \exp\left[j2\pi\left(\frac{\Delta f\cdot\ln(|n|+1)r_0}{c} - \frac{f_c R[1-\cos(n\cdot\Delta\beta)]}{c}\right) + w_{\text{opt}}\right] \quad (17)$$

The array factor AF of FDAA based on symmetric logarithm of nonlinear frequency and angular broadening null is:

$$\text{AF}(t,r,\alpha) = \sum_{n=-N}^{N} a'_n \exp\left[j2\pi\Delta f\cdot\ln(|n|+1)\left(t-\frac{r}{c}\right)\right] \exp\left[j2\pi f_c \frac{R\sin(n\cdot\Delta\beta)\sin\alpha_i}{c}\right] \quad (18)$$

4. SIMULATION RESULTS

4.1. Simulation Results of X-shaped Sidelobe Analysis of FDAA Beam Pattern

Assuming that the far-field target point is at $Q(r_0, \alpha_0)$, the simulation parameters are designed as shown in Table 1.

According to the simulation parameters set in Table 1, the nonlinear frequency offset of FDAA beam pattern is designed. As shown in Figure 3, when the total number of activated array elements K_A is 33, the influence of the scale coefficient q of the symmetric logarithm in the frequency offset design on the FDAA beam pattern is shown. Figure 3(a) is the FDAA beam pattern with $K_A = 33$ and the scale coefficient $q = 1$. Figure 3(b) is the FDAA beam pattern with the scale coefficient $q = 10$. By comparing Figure 3(a) with Figure 3(b), it is found that both of them form a point-like beam pattern, and the beam presents an 'X'-type crossover in the distance-angle

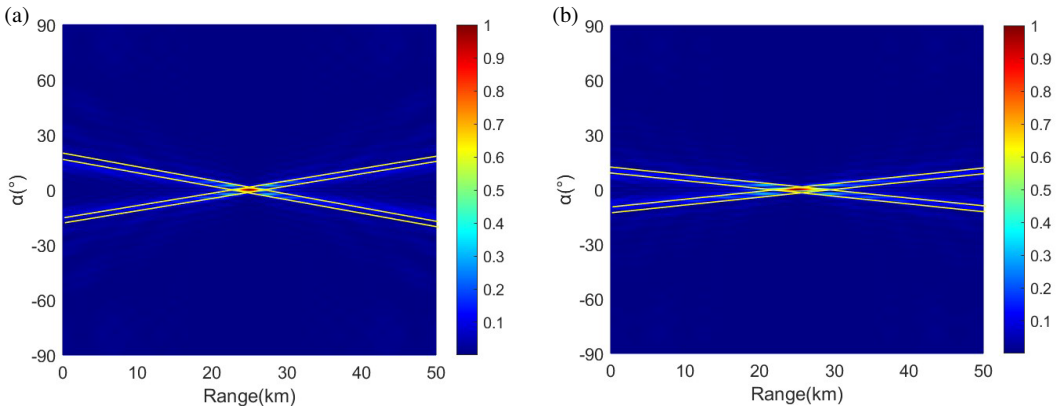

FIGURE 4. When $K_A = 67$, the influence of the scale coefficient q of the Sym-Log on the FDAA beam pattern.

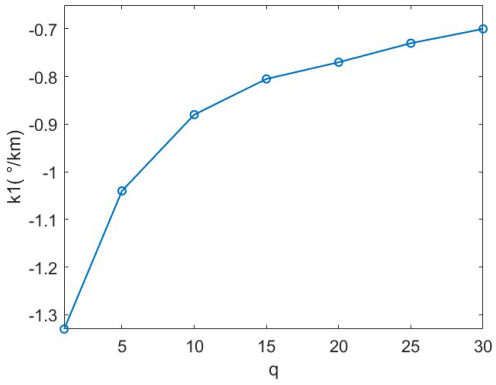

FIGURE 5. When $K_A = 33$, the curve of the beam slope k_1 changing with the scale coefficient q of the Sym-Log.

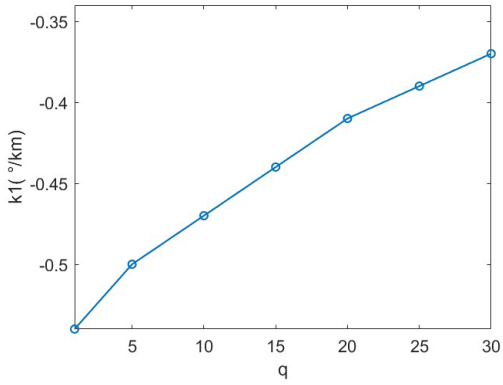

FIGURE 6. When $K_A = 67$, the curve of the beam slope k_1 changing with the scale coefficient q of the Sym-Log.

two-dimensional diagram. It can be seen that the angle formed by Figure 3(b) in the angle direction of the distance-angle two-dimensional diagram is smaller than that of Figure 3(a). As shown in Figure 4, when the total number of activated array elements K_A is 67, the influence of the scale coefficient q of the symmetric logarithm on the FDAA beam pattern is the same as that in Figure 4(a) and Figure 4(b). The beam also exhibits an 'X' -type crossover in the distance-angle two-dimensional diagram, and the angle formed in the angle direction of Figure 4(b) in the distance-angle two-dimensional diagram is smaller than that in Figure 4(a).

In order to analyze the influence of the scale coefficient q of the symmetric logarithm on the angle size, taking Figure 3(a) as an example, when the number of active array elements $K_A = 33$, two variables k_1 and k_2 are introduced to represent the relationship between the angle domain and the distance domain at any position of the strong sidelobe in the beam. k_1 represents the beam slope of the straight line L_1 downward along the beam direction; k_2 represents the beam slope of the straight line L_3 upward along the beam direction; k_1 and k_2 are opposite to each other, which will change with the change of the scale coefficient q. The line L_2 is parallel to L_1, and L_4 is parallel to L_3. It can be seen that the strong sidelobe position is mainly between L_1 and L_2, and between L_3 and L_4. The distance between L_1 and L_2 is about $1/4$ beamwidth. Therefore, it is better to suppress the interference position when the null width is set to $1/4$ beamwidth.

Assuming that the position of any interference signal on the beam between lines L_1 and L_2 is $P_1(\alpha_p, r_p)$, the beam slope k_1 can be expressed as:

$$k_1 = \frac{\alpha_p - \alpha_0}{r_p - r_0} \tag{19}$$

After calculation, as shown in Figure 5 and Figure 6, the curves of the beam slope k_1 change with the scale coefficient q of the symmetric logarithm when the number of activated array elements is $K_A = 33$ and $K_A = 67$, respectively. It can be seen that as the scale coefficient q of the symmetric logarithm gradually increases, the beam slope k_1 gradually increases and gradually approaches 0. Therefore, in the design of symmetrical logarithmic frequency offset, the scale coefficient q of symmetrical logarithm will have a certain influence on the beam pattern of FDAA in both range domain and angle domain. According to the relationship between the interference position and the expected target position in Formula (19), it can be seen that there is a certain relationship between the angle domain and distance domain at the interference position. The null set in the fixed direction is the null set at the interference position, so the null set at the fixed position in the distance domain can be calculated by Formula (19).

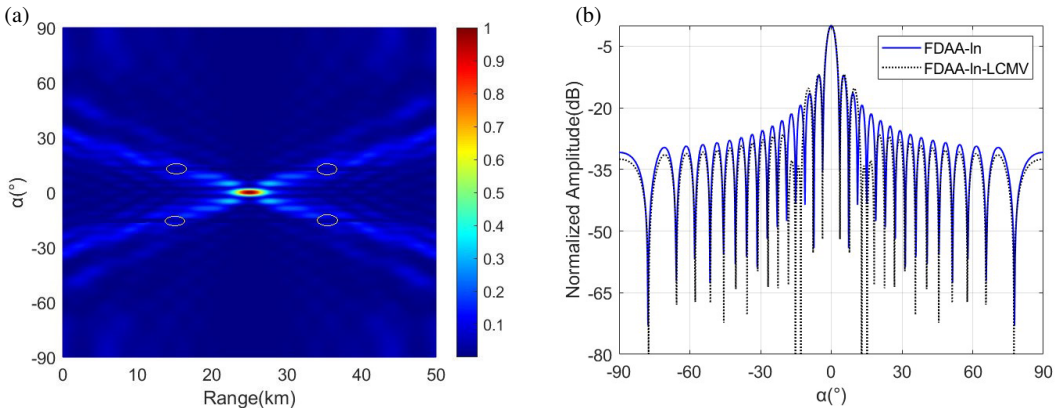

FIGURE 7. When $K_A = 33$, the angular domain broadened null FDAA beam pattern with the scale coefficient $q = 1$ in the frequency offset design is obtained.

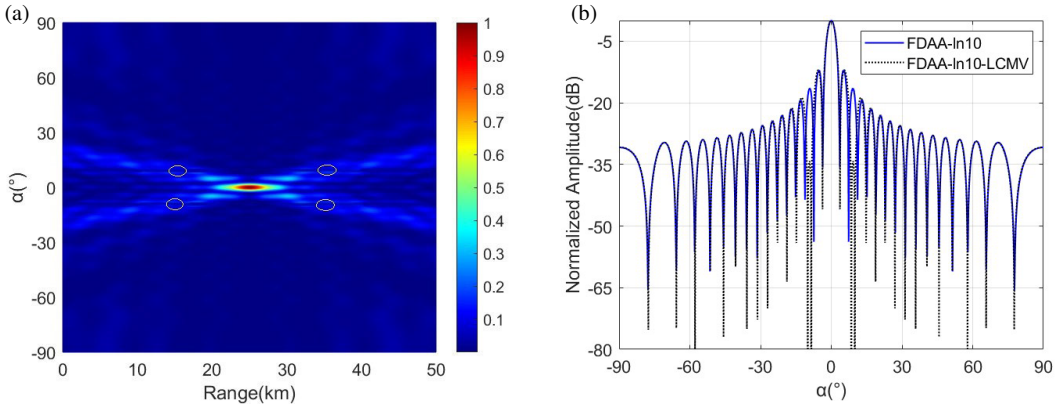

FIGURE 8. When $K_A = 33$, the angular domain broadened null FDAA beam pattern with the scale coefficient $q = 10$ in the frequency offset design is obtained.

4.2. The Simulation Results of Angular Broadening Null Beamforming for FDAA

When the total number of activated array elements K_A is 33, as shown in Figure 7, the angle domain broadened null FDAA beam pattern with the scale coefficient $q = 1$ is designed for the frequency offset. Figure 7(a) is the distance-angle two-dimensional simulation result diagram. It can be seen that a certain width of the notch is generated at the strong sidelobe interference in the fixed angle region. Figure 7(b) is the profile of nulling in the angle domain. Assuming that the null position is set at 36.4 km, 34.7 km, 15.3 km, and 13.6 km in the distance domain, the corresponding positions in the angle domain are calculated according to Formula (19) to be $-15.2°$, $-12.9°$, 12.9°, and 15.2°. It can be seen that the nulls with a depth about -34 dB are generated at $-15.2°$, $-12.9°$ and 12.9°, 15.2°. As shown in Figure 8, the null beamforming simulation diagram of symmetric logarithmic frequency offset with scale factor $q = 10$ is applied to FDAA in the angle domain. Supposing that the null position is also set at the distance domain of 36.4 km, 34.7 km, 15.3 km, and 13.6 km, the corresponding positions in the angle domain are calculated according to Formula (19) to be $-10°$, $-8.5°$, 8.5°, and 10°. As shown in Figure 8(b), a null with a depth about -33 dB is generated at $-10°$, $-8.5°$ and 8.5°, 10°. Therefore, it is verified by simulation that the sidelobe of FDAA can be suppressed by generating nulls at a fixed position in the angle domain.

Similarly, when the total number of activated array elements K_A is 67, as shown in Figure 9, the angle domain broadened null FDAA beam pattern with the scale coefficient $q = 1$ is designed for the frequency offset. Figure 9(a) is the distance-angle two-dimensional simulation result diagram. It can be seen that a certain width of the notch is generated at the strong sidelobe interference in the fixed angle region. Figure 9(b) is the cross-sectional view of the nulling in the angle domain. Assuming that the nulls are generated at the distance domain of 36.4 km, 34.7 km, 15.3 km, and 13.6 km, the corresponding positions in the angle domain are calculated according to Formula (19) to be $-6.2°$, $-5.2°$, 5.2°, and 6.2°. It can be seen that the nulls with a depth of about -37 dB are generated at $-6.2°$, $-5.2°$ and 5.2°, 6.2°. As shown in Figure 10, a null beamforming simulation diagram of symmetric logarithmic frequency offset with scale factor $q = 10$ is applied to FDAA in the angle domain. Assuming that the null position is set at 36.4 km, 34.7 km, 15.3 km, and 13.6 km in the distance domain, the corresponding positions in the angle domain are calculated according to Formula (19) to be $-5.4°$, $-4.6°$, 4.6°, and 5.4°. It can be seen that a null with a depth of about -38 dB is generated at $-5.4°$, $-4.6°$ and 4.6°, 5.4° in Figure 10(b). Therefore, in order to generate nulls for fixed-position sidelobes in the dis-

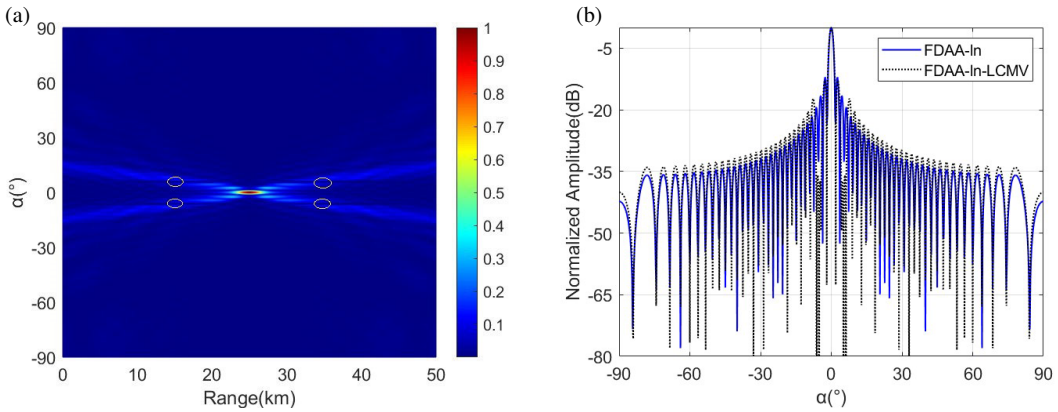

FIGURE 9. When $K_A = 67$, the angular domain broadened null FDAA beam pattern with the scale coefficient $q = 1$ in the frequency offset design is obtained.

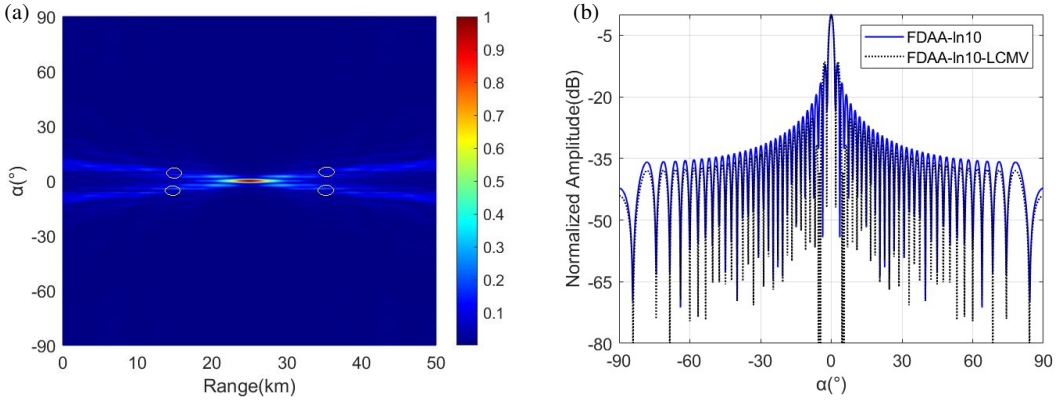

FIGURE 10. When $K_A = 67$, the angular domain broadened null FDAA beam pattern with the scale coefficient $q = 10$ in the frequency offset design is obtained.

tance domain, the position of the corresponding angle domain can be calculated by the formula, and null beamforming can be performed in the angle domain. The verification shows that the method can suppress the sidelobes.

5. CONCLUSION

This paper mainly analyzes the distribution of sidelobes after the nonlinear frequency offset design of FDAA. By studying the influence of the scale coefficient of the symmetric logarithm on the beam slope in the FDAA beam pattern, the position of the interference signal in the distance domain can be converted to the corresponding angle domain by the calculation formula and suppressed. In order to solve the interference problem caused by the fixed position sidelobe in FDAA, this paper proposes an FDAA with angular broadening null steering for sidelobe suppression. By setting a null with a certain width at the position of strong sidelobe interference in the angle domain, the strong sidelobe interference signal at any position generated by FDAA can be suppressed; the influence on the main lobe beam is reduced; the target beam is more concentrated; and the target recognition and tracking ability of the radar system is improved, which is conducive to the use of precision equipment such as spaceborne and airborne.

ACKNOWLEDGEMENT

This work was supported in part by National Natural Science Foundation of China under grant numbers 62071258, U22A2010 and 61971246.

REFERENCES

[1] Antonik, P., M. C. Wicks, H. D. Griffiths, and C. J. Baker, "Frequency diverse array radars," in *2006 IEEE Radar Conference*, 1–3, Verona, Ny, Apr. 2006.

[2] Ahmad, Z., M. Chen, and S.-D. Bao, "Beampattern analysis of frequency diverse array radar: A review," *Eurasip Journal on Wireless Communications and Networking*, 189, Nov. 2021.

[3] Wang, W.-Q., H. C. So, and H. Shao, "Nonuniform frequency diverse array for range-angle imaging of targets," *IEEE Sensors Journal*, Vol. 14, No. 8, 2469–2476, Aug. 2014.

[4] Sammartino, P. F. and C. J. Baker, "Developments in the frequency diverse bistatic system," in *2009 IEEE Radar Conference*, 1–5, Pasadena, CA, May 2009.

[5] Xu, J., G. Liao, S. Zhu, and H. C. So, "Deceptive jamming suppression with frequency diverse MIMO radar," *Signal Processing*, Vol. 113, 9–17, Aug. 2015.

[6] Secmen, M., S. Demir, A. Hizal, and T. Eker, "Frequency diverse array antenna with periodic time modulated pattern in range and angle," in *2007 IEEE Radar Conference*, 427–430, 2007.

[7] Khan, W., I. M. Qureshi, and S. Saeed, "Frequency diverse array radar with logarithmically increasing frequency offset," *IEEE*

Antennas and Wireless Propagation Letters, Vol. 14, 499–502, 2015.

[8] Gao, K., W.-Q. Wang, J. Cai, and J. Xiong, "Decoupled frequency diverse array range-angle-dependent beampattern synthesis using non-linearly increasing frequency offsets," *IET Microwaves, Antennas & Propagation*, Vol. 10, No. 8, 880–884, 2016.

[9] Wang, B., J. W. Xie, J. Zhang, and e. al., "Beamforming analysis based on CSB sin-FDA," *Journal of Systems Engineering and Electronics*, Vol. 31, No. 1, 73–84, Feb. 2020.

[10] Saeed, S., I. M. Qureshi, W. Khan, and A. Salman, "Tangent hyperbolic circular frequency diverse array radars," *The Journal of Engineering*, 23–28, 2016.

[11] Liao, Y., H. Tang, X. Chen, and W.-Q. Wang, "Frequency diverse array beampattern synthesis with Taylor windowed frequency offsets," *IEEE Antennas and Wireless Propagation Letters*, Vol. 19, No. 11, 1901–1905, Nov. 2020.

[12] Huang, G., Y. Ding, S. Ouyang, and V. Fusco, "Frequency diverse array with random logarithmically increasing frequency offset," *Microwave and Optical Technology Letters*, Vol. 62, No. 7, 2554–2561, Jul. 2020.

[13] Wang, W.-Q., M. Dai, and Z. Zheng, "FDA radar ambiguity function characteristics analysis and optimization," *IEEE Transactions on Aerospace and Electronic Systems*, Vol. 54, No. 3, 1368–1380, Jun. 2018.

[14] Higgins, T. and S. D. Blunt, "Analysis of range-angle coupled beamforming with frequency-diverse chirps," in *2009 International Waveform Diversity and Design Conference*, 140–144, Kissimmee, Fl, Feb. 2009.

[15] Gao, K., H. Chen, H. Shao, and J. Cai, "A two-dimensional low-sidelobe transmit beampattern synthesis for linear frequency diverse array," in *2015 IEEE China Summit & International Conference on Signal and Information Processing (ChinaSIP)*, 408–412, Chengdu, China, Jul. 2015.

[16] Gao, K., W.-Q. Wang, and J. Cai, "Frequency diverse array and MIMO hybrid radar transmitter design via Cramér-Rao lower bound minimisation," *IET Radar, Sonar & Navigation*, Vol. 10, No. 9, 1660–1670, Nov. 2016.

[17] Xu, W., L. Zhang, H. Bi, P. Huang, and W. Tan, "FDA beampattern synthesis with both nonuniform frequency offset and array spacing," *IEEE Antennas and Wireless Propagation Letters*, Vol. 20, No. 12, 2354–2358, Dec. 2021.

[18] Comisso, M., G. Buttazzoni, and R. Vescovo, "Reconfigurable antenna arrays with multiple requirements: A versatile 3D approach," *International Journal of Antennas and Propagation*, Vol. 9, 2017.

[19] Lan, L., G. S. Liao, J. W. Xu, and e. al., "Research on non-adaptive beamforming against main-lobe deception jamming for FDA-MIMO radar," *Signal Processing*, 944–950, 2019.

[20] Byun, G., H. Choo, and S. Kim, "Design of a small arc-shaped antenna array with high isolation for applications of controlled reception pattern antennas," *IEEE Transactions on Antennas and Propagation*, Vol. 64, No. 4, 1542–1546, Apr. 2016.

[21] Deng, Z., W. Xu, P. Huang, W. Tan, and Y. Qi, "Frequency diverse arc array beampattern synthesis analysis with nonlinear frequency offset," *Progress In Electromagnetics Research Letters*, Vol. 110, 109–116, 2023.

[22] Zhang, Y., "Research on clutter suppression method of airborne conformal array," Ph.D. dissertation, Xi'an University of Electronic Science and Technology, 2019.

[23] Xu, W., Z. Deng, P. Huang, W. Tan, and Z. Gao, "Beampattern synthesis and optimization for frequency diverse arc array based on the virtual element," *Electronics*, Vol. 12, No. 10, 2231, May 2023.